nature food

ARTICLES

https://doi.org/10.1038/s43016-021-00278-w

Solar geoengineering can alleviate climate change pressures on crop yields

Yuanchao Fan[1,2]✉, Jerry Tjiputra[1], Helene Muri[3], Danica Lombardozzi[4], Chang-Eui Park[5], Shengjun Wu[6] and David Keith[7,8]

Solar geoengineering (SG) and CO_2 emissions reduction can each alleviate anthropogenic climate change, but their impacts on food security are not yet fully understood. Using an advanced crop model within an Earth system model, we analysed the yield responses of six major crops to three SG technologies (SGs) and emissions reduction when they provide roughly the same reduction in radiative forcing and assume the same land use. We found sharply distinct yield responses to changes in radiation, moisture and CO_2, but comparable significant cooling benefits for crop yields by all four methods. Overall, global yields increase ~10% under the three SGs and decrease 5% under emissions reduction, the latter primarily due to reduced CO_2 fertilization, relative to business as usual by the late twenty-first century. Relative humidity dominates the hydrological effect on yields of rainfed crops, with little contribution from precipitation. The net insolation effect is negligible across all SGs, contrary to previous findings.

Climate intervention through solar geoengineering (SG) has been proposed as a complementary strategy for mitigating anthropogenic greenhouse gas-induced warming, particularly when discussing the ambitious climate target set in the Paris Agreement[1,2]. Solar geoengineering and related techniques typically use aerosols to counterbalance some of the radiative forcing from long-lived greenhouse gases, either by reflecting more shortwave solar radiation away from Earth via stratospheric aerosol injection (SAI)[3] or marine sky brightening (MSB; nomenclature in the Methods)[4,5], for example, or by enhancing Earth's longwave radiation towards space through cirrus cloud thinning (CCT)[5] (strictly CCT is not 'solar' but hereafter we will refer to all SG-related methods as SG). Although the number of modelling studies on the method and impact of SG technologies (SGs) has increased rapidly since Crutzen's 2006 paper[3], and the launch of the Geoengineering Model Intercomparison Project (GeoMIP)[6] in particular, the majority focused on the physical responses of the atmosphere, ocean and cryosphere components of the climate system to these large-scale interventions[7,8]. The impact of SG on terrestrial ecosystems and agriculture remains poorly understood[9]. Only a few modelling studies have so far investigated the regional[10–13] or global[14,15] impacts of a specific SG such as SAI on the yield of certain crops. Inconsistent findings on the mechanisms and effectiveness of SAI (for example the roles of temperature and radiation) on global crop yield have emerged in the literature[14,15], although these studies applied notably different approaches. A global assessment of agricultural responses to multiple SG methods, and a direct comparison of the agricultural impacts of SGs and CO_2 emissions reduction (ER) under similar radiative forcing pathways, were both needed.

We took a stepwise approach (Fig. 1a) to understand crop yield responses to our selected scenarios. We first implemented three SGs (SAI, MSB, CCT) on top of Representative Concentration Pathway 8.5 (RCP8.5) to achieve the same net reduction in radiative forcing as RCP4.5, which is then referred to as our ER scenario, using the NorESM1-ME climate model[16]. Each of the three SG methods has multiple design choices[17] that could result in different climate responses, but here we used one instance of an idealized experiment for SAI, MSB and CCT, respectively, and focused on cross-SG-method comparisons in our sensitivity analysis. We then applied the climate scenarios to the CLM5 process-based global gridded crop model[18] to determine the impact of SGs and ER on the yield of six major crops (maize, sugarcane, wheat, rice, soy and cotton) that produce food, bioenergy and fibre. For crop yield modelling, we note potential uncertainties with respect to changing land-use pathways under different emission scenarios[19]. According to a scenario matrix framework and the standard configuration in ScenarioMIP[20], we combined the RCP8.5 climate with Shared Socioeconomic Pathway 5 (SSP5) land use as the default configuration for RCP8.5. All of the SGs (SAI, MSB and CCT) and ER (represented by combining RCP4.5 climate with SSP5 land use, that is, $RCP4.5_{(SSP5LU)}$) scenarios were simulated with the same SSP5 land use as in RCP8.5 to exclude the effect of land-use change (LUC) in comparisons between SGs and ER (Supplementary Table 1). We performed additional simulations that apply combinations of climate, CO_2 and land use to isolate the physiological effect of CO_2 (with a special case of $RCP8.5_{(45CO2)}$ that combines RCP8.5 climate with RCP4.5 CO_2) and decompose climate-only effects (Fig. 1a), and to assess potential uncertainties associated with changing land use for ER (for example, from SSP5 to SSP2; Supplementary Sections 1 and 2).

Our results show that without mitigation, annual average warming over land and growing season warming over cropping areas

[1]NORCE Norwegian Research Centre and Bjerknes Centre for Climate Research, Bergen, Norway. [2]Center for the Environment, Faculty of Arts and Sciences, Harvard University, Cambridge, MA, USA. [3]Industrial Ecology Programme, Department of Energy and Process Engineering, Norwegian University of Science and Technology, Trondheim, Norway. [4]Climate and Global Dynamics Laboratory, National Center for Atmospheric Research, Boulder, CO, USA. [5]Department of Environmental Planning, Graduate School of Environmental Studies, Seoul National University, Seoul, Republic of Korea. [6]Three Gorges Research Center for Ecology and Environment, Chongqing Institute of Green and Intelligent Technology, Chinese Academy of Sciences, Chongqing, China. [7]John A. Paulson School of Engineering and Applied Sciences, Harvard University, Cambridge, MA, USA. [8]John F. Kennedy School of Government, Harvard University, Cambridge, MA, USA. ✉e-mail: ycfan@seas.harvard.edu

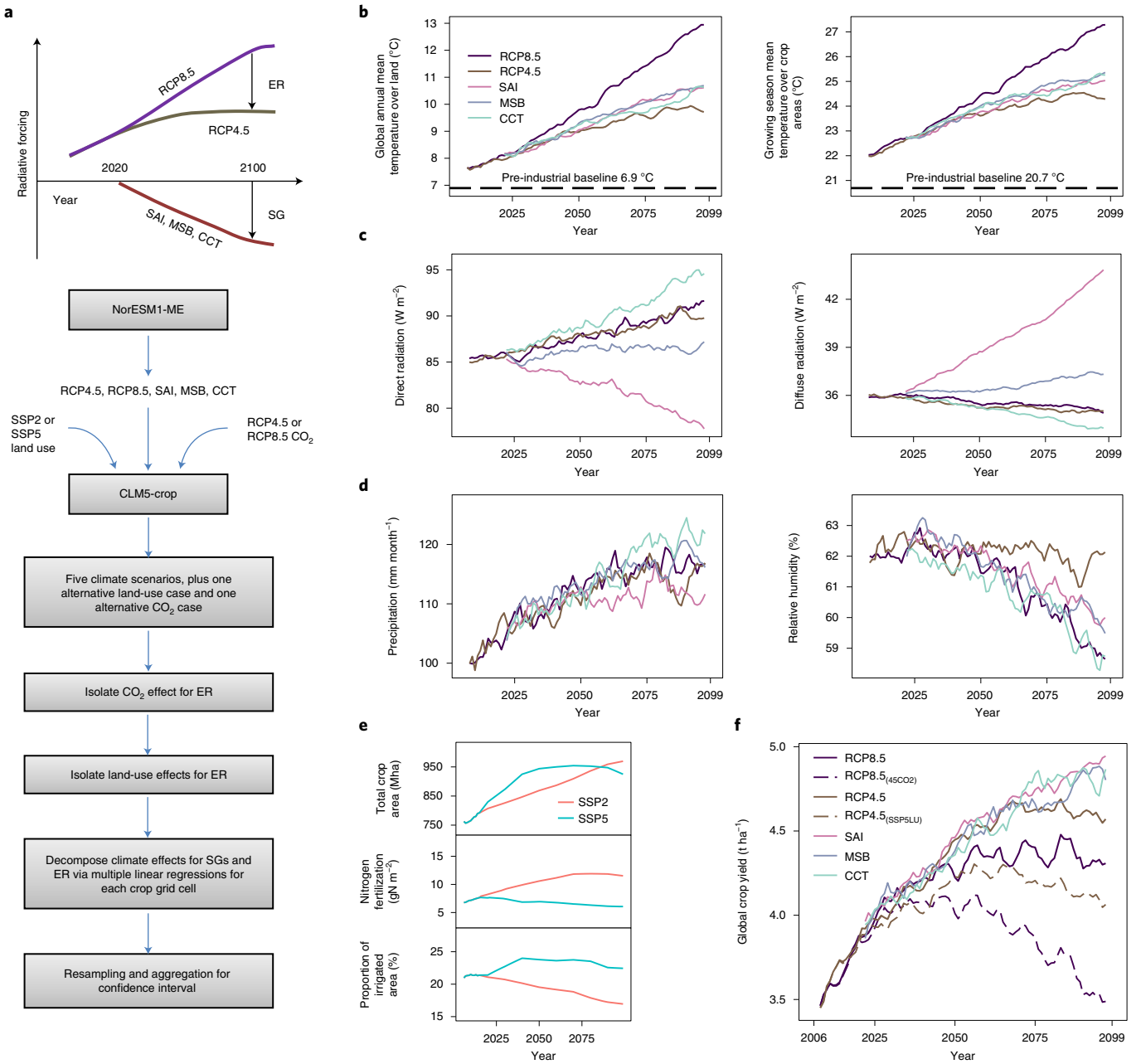

Fig. 1 | Methodology and global summary of key model variables. a, Experimental design of SGs and ER as alternative pathways to offset the anthropogenic radiative forcing from RCP8.5 down to RCP4.5 (top) and steps of climate and crop simulations and statistical analysis (bottom). All together, five climate simulations and seven crop simulations were performed (Supplementary Table 1). The statistical analysis focused on quantifying the partial and total climate effects under SGs and ER (compared to RCP8.5) by multiple linear regression (MLR). A special case of crop simulation RCP8.5$_{(45CO2)}$ was designed by combining RCP8.5 climate with RCP4.5 CO_2 to isolate the CO_2 effect for ER (see details in the Methods). The ER experiment RCP4.5$_{(SSP5LU)}$ used RCP4.5 climate and CO_2 and SSP5 land use. The comparison between RCP4.5$_{(SSP5LU)}$ and RCP4.5 (with SSP2 land use) was only meant to isolate potential LUC effects for ER but was not considered by SGs (see Sections 1 and 2 in the Supplementary Information). **b**, Air temperature time series (5-yr running means) of the global annual mean temperature over all of the land surface (left) and the growing season mean over crop areas only (right) simulated by NorESM1-ME. Dashed lines are pre-industrial (1850–1879 mean) values. **c**, Time series (5-yr running means) of global crop-area weighted-average growing season direct (left) and diffuse (right) solar radiation (in the visible band 0.3–0.7 μm only) simulated by NorESM1-ME. **d**, Time series (5-yr running means) of global crop-area weighted-average growing season precipitation (left) and relative humidity (right) simulated by NorESM1-ME. **e**, Annual total crop area (top), nitrogen fertilization (middle) and irrigation fraction (bottom) under land-use pathways SSP2 and SSP5. **f**, CLM5 simulated annual global crop yield (5-yr running means) in different experiments shown in Supplementary Table 1.

reach 5.4 °C and 6 °C, respectively, above pre-industrial levels by the end of the twenty-first century (2075–2099 mean; Fig. 1b), within the range of projections of the Fifth Assessment Report (AR5) of the IPCC[21]. Simulations show substantial changes in crop yields in response to changes in climate, CO_2 concentration, land-use and crop management trends under the different scenarios (global trends in Fig. 1f and crop-specific trends in Supplementary Fig. 1). We validated CLM5 modelled crop yields during the period

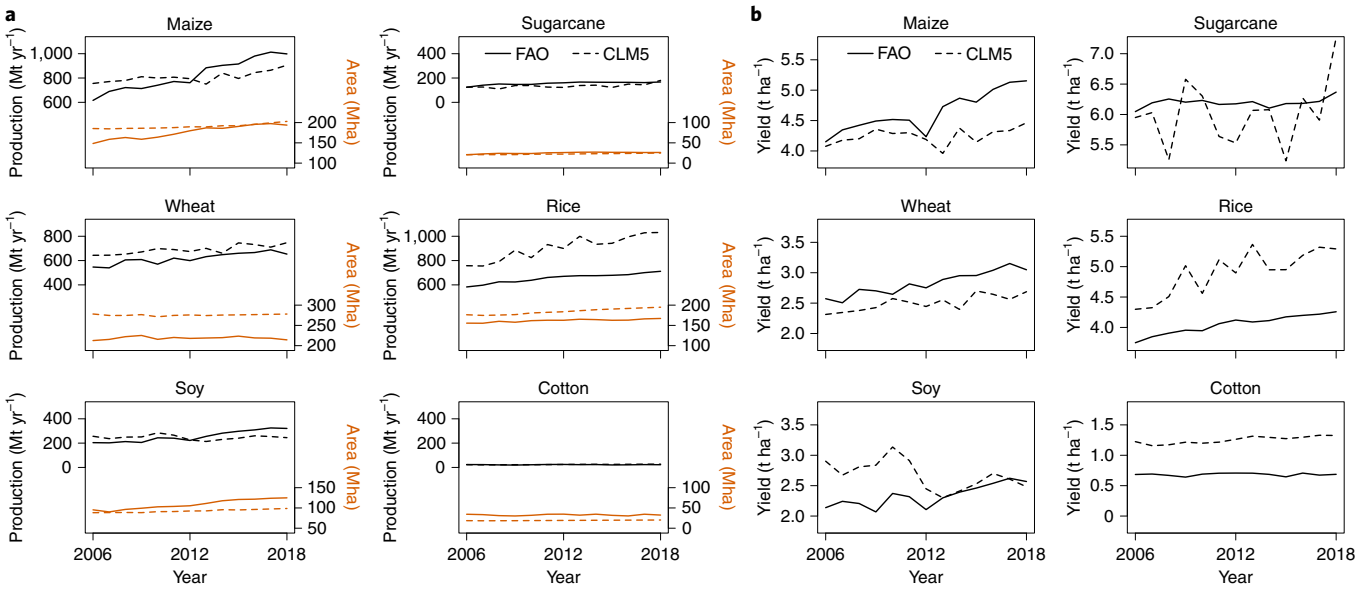

Fig. 2 | Validation of CLM simulated crop production and yields for the recent past with FAO data. a, Comparison of annual production and cultivation area for the six crops between CLM5 and FAO data for the period 2006–2018. **b**, Model–data comparison of per-hectare yields.

2006–2018 with FAOSTAT data[22], which showed reasonable fidelity in simulated levels of global total production and average yields (Fig. 2). More detailed global and regional evaluation of CLM5 crop simulations can be found in Lombardozzi et al.[18].

We quantified the relative effects of surface air temperature, direct and diffuse solar radiation, precipitation and relative humidity on each crop type under each of the SG and ER scenarios compared with RCP8.5 by conducting multiple linear regression (MLR) for each grid cell and each crop type on 2020–2099 time-series data. We found the mean partial and total climate effects for the globe, and then used a Monte Carlo or bootstrap approach[23] to resample and derive a confidence interval for each MLR coefficient (Fig. 1a; details in the Methods). To estimate the net impact of ER, the climate-only effects were merged with the effect of reduced CO_2 from RCP8.5 to RCP4.5. Finally, we compared SGs and ER to assess the mechanisms and effectiveness of the different scenarios for agricultural production in the twenty-first century.

Partial and total climate effects

The different cooling strategies result in spatially and temporally heterogeneous impacts on crop yield in the twenty-first century (Figs. 3–5). Reduced air temperature has consistently strong positive effect on global average yield under all scenarios (Fig. 3). In contrast to the similar temperature effects, the different scenarios offer distinct radiation and moisture-related effects and trends across regions and over time. The moisture effect, dominated by changes in relative humidity rather than precipitation, drives much of the interannual variability in the total climate effect. Remarkably, in ER it reaches a comparable level to the temperature effect after year 2050 (Fig. 3d). The net effect of relative humidity is closely linked to the vapour pressure deficit, which is important for crop growth and yield[24,25]. There are simultaneous drops in precipitation and relative humidity around the year 2067 under RCP8.5, indicating a dry period (Fig. 1d). The SGs and ER scenarios all have increased relative humidity compared with RCP8.5 around 2067. Increased relative humidity reduces the vapour pressure deficit and alleviates water stress, which explains the synchronous peak of the relative humidity effect under all scenarios during this dry period (Fig. 3a–d). The net effect of altered radiation regimes on crop yield is relatively small in all scenarios, owing to the opposing changes in the direct and diffuse radiation components. Under SAI, the positive effect of increased diffuse radiation on yields largely compensates for the loss caused by reduced direct sunlight, and in some cases contributes to increased yields (Fig. 3a,e). In CCT, contrastingly, the slight increase in direct radiation versus decrease in diffuse radiation from the reduced layer of thin ice clouds in the upper troposphere brings a marginal net increase in global yields (Fig. 3c,e). MSB shows weaker radiation effects than SAI (Fig. 3b,e), given that the aerosol forcing is applied only over the oceans.

Crop-specific analysis shows diverse responses of the six crops to changes in different climate variables. The yield increments of most crops are primarily driven by cooling (Fig. 4). The exceptions are wheat and rice, which are particularly insensitive to temperature (Supplementary Fig. 1) yet respond strongly to changes in radiation and relative humidity under ER, SAI and MSB when not irrigated (Fig. 4a). Separating irrigated and rainfed crops shows that the effects of temperature and radiation are dependent on water stress levels. Eliminating water stress through irrigation dampens the effects of temperature and radiation for most crops, and for some crops reduces the total effect by more than 50% (Fig. 4a,b). Most rainfed crops show significant responses to increased relative humidity, with larger increases under ER than SGs (Figs. 3 and 4a). CCT shows a muted crop relative humidity response (Figs. 3e and 4a) because it causes only small changes in global average humidity compared to RCP8.5 after 2075 (Fig. 1d). Precipitation exerts minimal effects on most rainfed crops after accounting for temperature, radiation and relative humidity effects, which holds even if relative humidity is removed from the regression (equation (1)). The minor role of precipitation reflects the complexity of crop water availability and use due to variable runoff, drainage and evaporation[26]. As relative humidity regulates evaporation and plant water use through stomatal control, increased relative humidity alleviates water stress for rainfed crops at a given temperature; lower relative humidity indicates a higher vapour pressure deficit, which may trigger stomatal closure[25,27,28] and reduces crop growth and yield[26]. Our finding of the dominant role of relative humidity rather than precipitation on crop productivity is consistent with a previous SAI study that considered both variables[11] (other SAI studies neglected relative humidity[10,14,15]) and with other studies on the role of relative humidity or the vapour pressure deficit on vegetation and crop productivity[24,25,27].

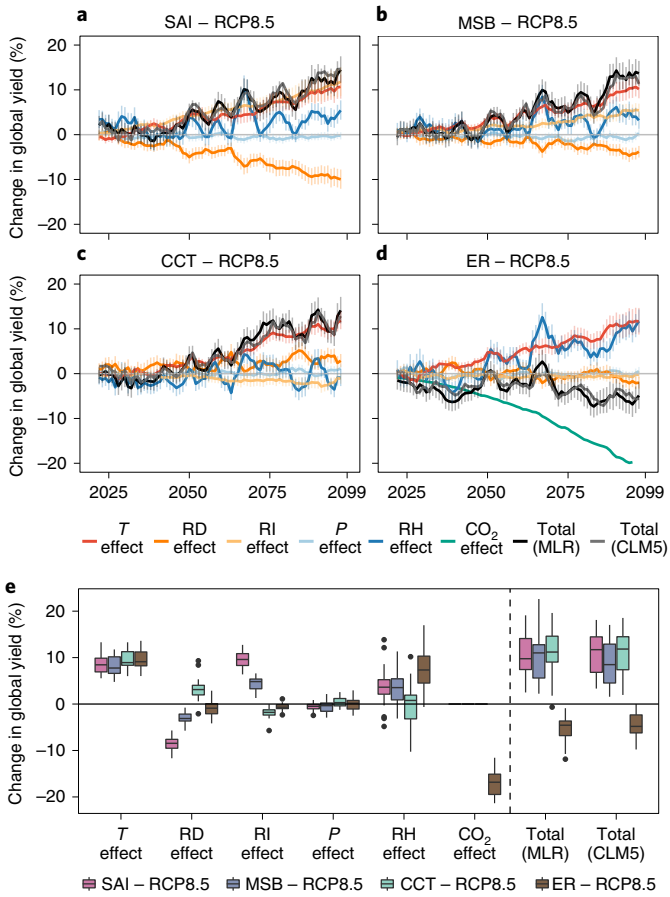

Fig. 3 | Partial and total effects of SG or ER on global crop yield. **a**–**d**, Time series (5-yr running means) of partial climate effects decomposed by MLR analysis, the isolated CO_2 effect for ER, and MLR-predicted and CLM5 modelled total effects under SAI (**a**), MSB (**b**), CCT (**c**) and ER ($RCP4.5_{(SSP5LU)}$; **d**) relative to RCP8.5 in the twenty-first century. The CO_2 effect is not shown in **a**–**c** as it is not relevant for SGs. Coloured lines indicate the mean effects and error bars indicate the 2.5–97.5 percentile confidence interval for MLR predictions (only the means are shown for the CLM5 modelled total effect and CO_2 effect). *T*, temperature; RD, direct radiation; RI, diffuse radiation; *P*, precipitation; RH, relative humidity. **e**, Box plot of the mean partial and total effects for the period 2075–2099 (the lower and upper edges of the box are the first and third quartiles, the horizontal line is the median and the whiskers show 1.5× the interquartile range; points beyond the ends of the whiskers are outliers). Global yields are crop-area weighted averages across the six crop types. The difference between the MLR estimated total effect and CLM5 modelled total effect indicates the residual errors (average −0.8%, 1.1%, 0.3% and −0.6% for the SAI, MSB, CCT and ER scenarios, respectively, during 2075–2099).

Overall, the methods that promote cooling and at the same time alleviate water stress, which occurs in Central America and South America in most scenarios (Supplementary Fig. 2), will probably result in the highest yield gains, particularly for maize, soy and sugarcane in the Global South (Fig. 5 and Extended Data Figs. 1 and 2). Globally, higher relative humidity increases yields by ~3% under the SGs and 8% under ER (2075–2099 mean). By comparing the different SGs and ER, our results suggest that evaluating climate impacts on water availability and agricultural productivity should not focus only on precipitation, but instead on the balance of water input and water loss. Taking relative humidity into account forces a re-evaluation of previous assessments that SAI would have a negative impact on crop yield due to reduced precipitation[7,10]; we found little impact of precipitation reduction in India and China, and even yield increases in South America.

Reduced CO_2 fertilization under ER

The combined cooler temperatures and higher humidity under ER (Fig. 1) would lead to increased global yields compared with the SG scenarios if one neglects the impact of CO_2 fertilization (that is, $RCP4.5_{(SSP5LU)} - RCP8.5_{(45CO2)}$). However, the reduced crop yields because of lower CO_2 concentrations under ER outweigh the temperature and humidity benefits regionally (Extended Data Fig. 1d) and globally (Figs. 3 and 4) for most C_3 crops, resulting in a global marginal loss of yield by −5% during 2075–2099 ($RCP4.5_{(SSP5LU)}$ – RCP8.5; Fig. 3e and Supplementary Table 2). Our regression analysis shows that doubling CO_2 concentration from 380 to 760 ppm while other climate variables remain the same as RCP8.5 increases global yields by 9%, 16%, 20%, 25% and 31% for maize, sugarcane, rice, cotton and wheat, respectively, and up to 75% for soy (Methods and Extended Data Fig. 3). These CO_2 fertilization factors, except for soy, are very similar to those used in the DSSAT model and related SG studies[10,14] and those observed in the Free-Air CO_2 Enrichment (FACE) experiments (per 200 ppm CO_2 increment)[29,30]. Although elevated CO_2 can stimulate soy's photosynthetic capacity by 60–80% as it is not limited by nitrogen, several plant-level physiological feedbacks limit soy's investment for reproduction and thus reduce the yield sensitivity[31], but this mechanism is not included in CLM5. Halving the yield response of soy to CO_2 would make it closer to observations and other crops (Extended Data Fig. 3) but does not change our conclusion on the comparative effects of ER and SG. The higher sensitivity of C_3 crops (soy, wheat, rice and cotton) to CO_2 concentrations than C_4 crops (maize and sugarcane) is consistent with observations[32], although notable spatial heterogeneity exists even for a given crop type (Extended Data Figs. 1 and 2), which is probably related to changing soil nutrient and moisture conditions[33]. A comparison of irrigated and rainfed crops reveals that eliminating water stress via irrigation reduces the CO_2 effect for most crops (Fig. 4); this is related to the role of elevated CO_2 in improving plant water-use efficiency (and vice versa) and consistent with observations of the effect of CO_2 on crops decreasing with higher water availability[30].

Our quantitative analysis shows that the reduced CO_2 fertilization under ER undermines its cooling and humidity benefits, making SGs robustly more effective at increasing global yields (11%, 9% and 11% for SAI, MSB and CCT, respectively, during the period 2075–2099; Fig. 3e and Supplementary Table 2), although they have distinct mechanisms.

Limitations and uncertainties

Our results are only as good as our assumptions. The use of any SG technology would entail many design choices that would shape the spatial and temporal distribution of radiative forcing, along with many of its side effects[17]. The spatial distribution of sensitivity to MSB and CCT interventions in particular depends on aerosol–cloud interactions that are poorly constrained by observations[34]. The meridional distribution of SAI is a design choice with important consequences for hydrology[35].

NorESM1-ME showed satisfactory performance on climate projections in CMIP5[36] and GeoMIP5[37] and CLM5 has also been rigorously evaluated[18,38,39]. Nevertheless, the absolute prediction of future crop yields is hindered by uncertainties in estimating future climates or in the forcing dataset[40], in the crop model parameterizations[18] and in assumptions regarding country-specific differences in agricultural practice and adaptation[41]. The CLM5 crop model needs improvements in allocation and temperature-triggered phenology, as well as biological nitrogen fixation for soy[18], and can be further improved towards better representation of crop response to extreme weather events[42] and to CO_2 fertilization. Lombardozzi et al.[18] showed that the CLM5 simulated crop yield response to CO_2

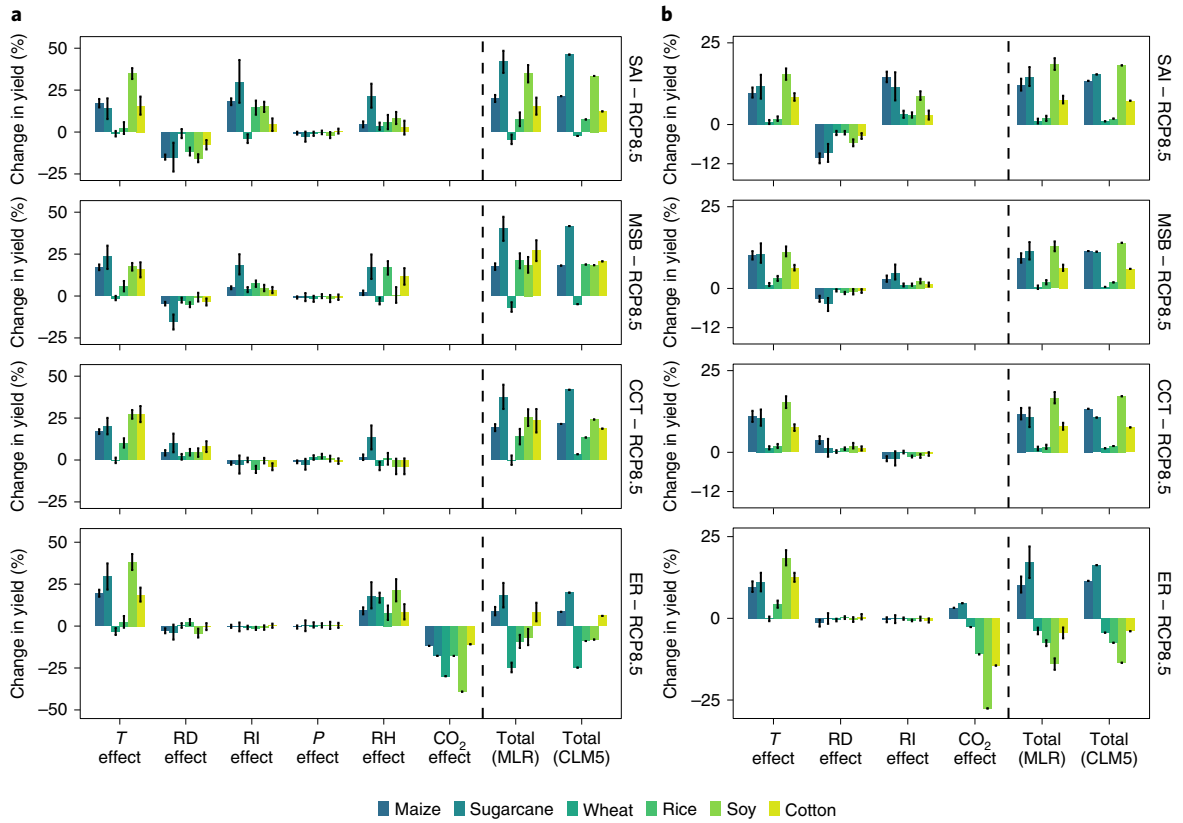

Fig. 4 | Global partial and total effects of SG or ER on yield for each crop type. a, Change in yield for rainfed crops considering all climate variables (abbreviations as in Fig. 3) and CO_2 (for ER) relative to RCP8.5. **b**, Change in yield for irrigated crops without *P* and RH (Methods). Error bars indicate the 2.5–97.5 percentile confidence interval averaged over the period 2075–2099. Note that the *y*-axis ranges of irrigated crops (**b**) are only half of those of rainfed crops (**a**), suggesting a much weaker sensitivity of irrigated crops. The difference between the MLR estimated total effect and CLM5 modelled total effect indicates the residual errors (−1.0%, −3%, −1.8%, 0.6%, 1.0% and 4.0% in **a**, and −1.5%, 0.1%, 0.1%, −0.04%, −0.4% and 0.1% in **b** for maize, sugarcane, wheat, rice, soy and cotton, respectively, averaged across the scenarios during 2075–2099).

enrichment was nearly double observations from FACE experiments[29] and the higher responses of irrigated crops than rainfed crops was the opposite of observations. But our independent evaluation of CLM5 against observations shows reasonable CO_2 effects for most crops (except for soy) whether irrigated or not. There are several reasons for this difference, including different forcing data and different climate contexts of evaluation: Lombardozzi et al.[18] used the GSWP3 forcing for a historical scenario (added 200 ppm CO_2 from 1990 to 2010 while other climate variables remained the same), whereas our simulations used coupled model forcing for future scenarios. Moreover, we found abnormal sub-daily covariance of surface air temperature and relative humidity in the GSWP3 dataset resulting in substantially higher moist heat stress (measured by wet-bulb temperature[43]) for tropical, subtropical and some mid-latitude regions than several other reanalysis datasets (not presented here). The abnormal forcing data used in Lombardozzi et al.[18] could affect the energy and water cycle in CLM5[40] and contribute to the differences in simulated yield responses to CO_2 compared with our crop simulations, which are more consistent with observations. In CMIP5[36] coupled simulations, the CLM model showed a weaker land carbon response to CO_2 than other land surface schemes, and CLM5 has an improved response to CO_2 compared with older versions of CLM[44].

Could our model underestimate the effect of dimming for SAI? One must consider the radiative properties of aerosols when assessing the impact of SAI. The same increase in stratospheric aerosol optical depth (SAOD) could produce different amounts of downscattering depending on the aerosol size distribution. All else equal, a higher diffuse radiation fraction enhances canopy absorption of photosynthetic active radiation[45] and carbon uptake in forests and croplands[46], and also promotes crop yields due to enhanced radiation-use efficiency[47]. Thus, per unit increase in SAOD, the SAI with relatively more downscattering aerosols and a higher proportional increase in diffuse radiation should have larger yields. Proctor et al.[15] examined observations of SAOD and crop yields, finding a strong net negative insolation effect offsetting the positive cooling effect of SAI on crop yields. Their study rested on two important assumptions: (1) a homogeneous linear insolation effect of SAOD taken from the Pinatubo eruption (which had less downscattering than other volcanic eruptions such as the El Chichón eruption[15], and less than our model SAI experiment); (2) their reference scenario was RCP4.5 instead of RCP8.5, and thus their cooling effect of SAI was weaker than our case. Our sensitivity analysis of modelled crop responses to radiative changes (Extended Data Fig. 4) showed that the negative effect of reduced direct radiation could overtake the positive diffuse radiation effect if the direct and diffuse components decrease (for example, −20%) and increase (for example, +20%) proportionally. When applying our MLR coefficients to volcanic-induced changes in direct and diffuse radiation after the Pinatubo eruption (−21% direct and +20% diffuse, from Proctor et al.[15]), we found similar net negative insolation effects on maize (−8.9%), rice (−6.7%), soy (−3.6%) and wheat (−2.7%) to those shown in fig. 3 of Proctor et al.[15]. In our SAI experiment, the non-proportional opposing changes in direct (−11 W m^{-2} or −12%) and diffuse (+7 W m^{-2} or +20%, 2075–2099 mean) radiation relative to RCP8.5 (Fig. 1c) indicate more downscattering, resulting in

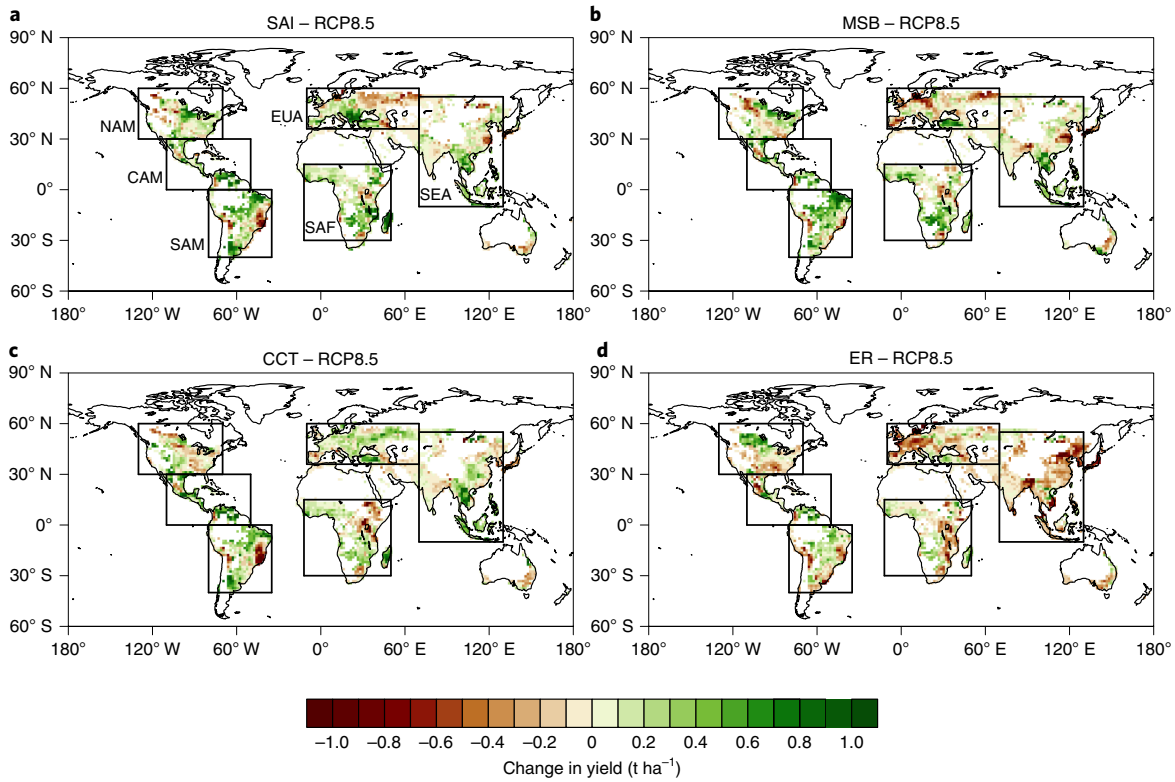

Fig. 5 | CLM5 simulated changes in global crop yields under SG or ER. a–d, Absolute changes in yield under SAI (**a**), MSB (**b**), CCT (**c**) and ER (RCP4.5$_{(SSP5LU)}$; **d**) compared with RCP8.5 (2075–2099 mean). The six region boxes indicate North America (NAM), Central America (CAM), South America (SAM), Europe and Western Asia (EUA), Southeast Asia (SEA) and Central and Southern Africa (SAF). This figure (including the background continental outlines) was prepared with the NCAR Command Language[59].

negligible net insolation effects on most crops (Fig. 4), although small regional variations exist (Extended Data Figs. 1 and 2). We also found that the effects of opposing changes in direct and diffuse radiation largely would cancel out each other in MSB and CCT scenarios. Therefore, the difference between our results and those of Proctor et al.[15] is not due to differences in crop sensitivity to the radiative changes in CLM5 versus observations, but is instead mainly due to different radiative changes in our SG experiments from those after the Pinatubo eruption. Our study highlights the importance of optimizing the aerosol particle size distribution. Given that the increase in diffuse light from SAI is somewhat adjustable through design choices[48], the impacts of a particular volcanic eruption are a limited analogue for SAI deployment.

Besides the physiological responses of crops to climate and CO_2, agricultural management such as irrigation and nitrogen fertilization are known to impact crop productivity[49], but have not been fully considered in previous SG studies. Our goal was to isolate the effect of ER (climate and CO_2 only) on crop yields. But ER will probably be linked to changes in land use, although future land-use and agricultural practice are hard to predict under any mitigation scenario. We examined the potential importance of LUC by adopting the IPCC standard, in which RCP8.5 is associated with SSP5 and RCP4.5 with SSP2[20]. Under these conditions, the relative advantage of SGs over ER in terms of effect on global average yields (Supplementary Fig. 3a) and on global total production (Supplementary Table 2) become smaller but still robust. This is mainly due to higher nitrogen fertilizer use in SSP2 than SSP5 (Fig. 1e) to balance the demands for food, feed and bioenergy production with limited land area available for agriculture[50], which largely compensates for the weaker CO_2 fertilization effect in ER for most crops (Supplementary Fig. 3b,c). In our LUC analysis, the yields of most crops except soy and cotton were sensitive to increased nitrogen fertilizer usage (Supplementary Fig. 4). Other confounding factors in crop responses to LUC include the effective climate shift caused by changing the spatial distributions of crops from SSP5 to SSP2 (Supplementary Figs. 5 and 6) and changing the irrigated fraction of each crop type (Fig. 1e and Supplementary Figs. 7 and 8). The LUC analysis implies that the advantage of SGs over ER depends on the assumption that their use is not associated with other management or technological changes that might increase or reduce crop yields.

Conclusions

Cooling is the primary driver of increases in crop yields under both SG and ER relative to RCP8.5. An important secondary driver is the interannual variability in relative humidity under different scenarios. The strong cooling and humidity benefits under ER are counteracted by its reduced CO_2 fertilization, leading to reduced yields compared with the SGs. The net impact of changes in direct and diffuse radiation is small under all scenarios. Overall yields in the Global South benefit consistently from all scenarios, particularly for maize, soy and sugarcane, whereas wheat and rice are less sensitive to the cooling induced by SGs or ER in general.

Our conclusions depend on other unaddressed uncertainties in the models. Future efforts could extend this assessment by using different climate and crop models and forcing datasets. Climate mitigation ultimately depends on synergistic efforts from all social-economic sectors, considering the advantages of multiple solutions and their potential risks. Policymakers should seek a balanced approach to sustaining global production of food, bioenergy and fibre, considering the various effects of different mechanisms offered by SGs and ER in regulating the carbon, water and nutrient cycles in agricultural systems.

Methods

Among the GeoMIP5 models, the three SGs (SAI, MSB, CCT) were simulated consistently only in the Norwegian Earth System Model version 1 (NorESM1-ME), providing a unique experiment set for comparing multiple SG methods in this study. Even the current GeoMIP6 does not have consistently designed experiments for SAI, MSB and CCT like those done in NorESM1-ME. The general climate features under three SGs, together with RCP4.5 and RCP8.5, have been thoroughly analysed in previous studies[5,8,51]. Details of SG implementations can be found in Muri et al.[5]. In the MSB experiment, sea salt emissions were increased in both clear-sky and cloudy regions to actively draw on the direct effect of sea salt aerosols in addition to the indirect effect through marine cloud processes, which is thus referred to as marine sky brightening instead of more commonly studied marine cloud brightening[1,4]. We note that each SG method itself has multiple design choices that could result in different climate and crop yield responses. Such intramethod variations for a specific SG technique is beyond the scope of this study and we focused on cross-SG-method comparison for our yield impact analysis. Here we reran these simulations with the output of high-frequency (1 h to 3 h intervals) coupler history data to force the crop model. We chose the Community Land Model version 5 (CLM5) as the crop model because CLM4 (within NorESM1-ME) does not have the prognostic crop types required for this study. CLM5 is a global land model that represents changing distributions of multiple crop types and management through time[18]. This enabled us to simulate transient yields of the six common crops under different climate and land-use scenarios.

Model experiments. We used the fully coupled emission-driven NorESM1-ME climate model to simulate the three SG scenarios (SAI, MSB and CCT) from 2020–2099, as well as two reference climate scenarios (RCP4.5 and RCP8.5) from 2006–2099 at 1.9° latitude × 2.5° longitude resolution. The SAI, MSB and CCT schemes were implemented on top of an RCP8.5 baseline in a consistent manner, such that the change in radiative forcing in RCP8.5 was reduced to that comparable to the RCP4.5 scenario (ER) during the period 2020–2099. The NorESM1-ME coupler history data for these five climate scenarios were downscaled to 0.9° latitude × 1.25° longitude resolution and then used as meteorological forcing to drive CLM5 with prognostic crops (CLM5-crop). CLM5-crop represented the growth, yield and agricultural management of six major crops: maize, wheat, rice, soy, sugarcane and cotton. Each crop was split into irrigated and rainfed subtypes, varying by region. Soy and maize also have temperate and tropical cultivars, which were merged in the post-processing before the analysis. The Land-Use Harmonization (LUH2) transient land-cover data[52] provided yearly surface boundary conditions of SSP2 and SSP5 scenarios at 0.9° latitude × 1.25° longitude resolution. All crop simulations of SGs and ER used the SSP5 land use as in RCP8.5 to facilitate interscenario comparison for quantifying the effects of changes in different climate variables on crop yields. We also set up two offline crop simulations: one combined RCP8.5 climate and RCP4.5 atmospheric CO_2 concentrations to isolate CO_2 effects, and another combined RCP4.5 climate and SSP2 land use to represent a scenario in which ER is associated with changing land use and related effects (compared with RCP8.5). We conducted a total of seven CLM5 crop simulation experiments, as summarized in Supplementary Table 1, which output yield data for each of the six crop types and for rainfed and irrigated subtypes separately.

Crop model evaluation. CLM5 simulated crop production and per hectare yields were compared with FAOSTAT data[22] from 2006 to 2018 (Fig. 2). The FAO crop production quantities were first converted to dry matter using crop-specific dry-to-fresh weight ratios[53]. Sugarcane yields were expressed as the amount of sucrose after dividing FAO cane yields by a tonnes cane per tonne sugar ratio of 8. Cotton yields represent cotton lint production divided by its harvested area. CLM5 modelled crop harvest amounts (in $gC\,m^{-2}$) under RCP8.5 from 2006–2018 were converted to dry matter using a carbon-to-dry-weight ratio of 0.45 and a harvest efficiency of 85% according to the CLM5 tech note (https://escomp.github.io/ctsm-docs/doc/build/html/tech_note/). Overall, the cumulative production ($Mt\,yr^{-1}$) simulated for most crops was within ±20% of the FAO data, with the exception of rice, for which the overestimation exceeded 30%. Biases existed in the crop cultivation area of SSP5 land-use time-series data for years 2006–2018 compared with the harvested area of FAOSTAT, especially for wheat and cotton, although their simulated productions were close to observation (Fig. 2a). Overall, the simulated yield per hectare aligned reasonably well with FAO data (Fig. 2b). For soy and rice, the overestimation was less than 20% in the validation period, and for maize, wheat and sugarcane the underestimations were less than 12%. The larger overestimation for the cotton yield (80%) was due to its smaller cultivation area but similar simulated production in CLM5 compared with FAO records.

Decomposing climate effects per crop type. We used MLR for each 0.9° × 1.25° grid cell and each crop type to determine how SG- or ER-induced changes in different climate variables contributed to yield change with reference to RCP8.5 during the intervention period 2020–2099:

$$\log(Y_i) - \log(Y_c) = \beta_0 + \beta_i (X_i - X_c) + \epsilon \quad (1)$$

where Y is the CLM5 modelled yield, $\boldsymbol{\beta}$ is a vector of coefficients (β_0 for the intercept) and $\mathbf{X}$ is a vector of explanatory variables including surface air temperature (T), direct solar (RD) and diffuse (RI) radiation, precipitation (P) and relative humidity (RH), all growing season means based on each crop's planting dates. ϵ is the residual error for any factors not captured by the explanatory variables. Subscript i indicates one of the SGs (SAI, MSB, CCT) or ER ($RCP4.5_{(SSP5LU)}$) simulations and c indicates the control simulation, which is RCP8.5 for the SGs but $RCP8.5_{(45CO2)}$ for the ER, such that all scenarios have the same land-use and CO_2 pathways to decompose climate-only effects. We focused on the transient effects of changes in climate due to SG or ER on yield in relative terms, $(\log(Y_i) - \log(Y_c) = \log\left(\frac{Y_i}{Y_c}\right)$, because yields followed a log-normal distribution[54]. In this way, our statistical analyses focused on the relative impacts of per unit change in climate variables on each crop no matter what the base yields were across grid cells and regions. We tested the sensitivity of irrigated crops to P and RH and found no significant effects, because irrigated crops received adequate water to reduce water stress every day in the CLM5 (applying unlimited water to offset the soil moisture deficit of the irrigated crop columns at 6:00 local time). Thus, for irrigated crops, the terms for moisture (P, RH) were excluded from the regression.

We conducted the MLR for each crop using equation (1) at each grid cell if the specific crop's cultivation area exceeded 1,000 ha in that cell for more than 60 yr between 2020 and 2099 (that is, 6,641 unique grid cells contributing to 23,928 crop-grid specific regressions, with each MLR based on a one-dimensional time series of $60 \leq n \leq 80$). Although land-use data were identical between the experimental (i) and control (c) simulations, due to crop distribution changes across years, some grid cells that did not meet the above criteria were excluded from the MLR for each specific crop. Grid cells with crop failures (zero or small yield values) in some years were set with a minimal yield for each crop type according to its 5th global percentile. The average crop failure rates were 3.5% for RCP8.5, 3.7% for RCP4.5, 3.5% for SAI, 3.5% for MSB and 3.4% for CCT. Setting a minimal yield was not only intended to ensure valid values of log(yield) but also to include crop failure related to extreme events. We checked the variance inflation factor (VIF) for multicollinearity among independent variables. The majority of grid-cell-level MLRs (98%) had VIF < 10 (low multicollinearity) for all independent variables. Removing the 2% grid cells with VIF > 10 did not affect the predicted relative contribution of partial climate effects, but would have slightly biased the MLR-predicted total effect compared with the original CLM5 modelled global average yield change. Thus, all the grid-cell-level regressions were included in the final analysis. We tested interaction effects between T and RH and between RH and P in the MLR. The Akaike information criterion (AIC) score showed that only one interaction term between T and RH improved the model fit slightly, but was only significant for sugarcane under SAI (Extended Data Fig. 4). RH and P had no obvious interaction effect. We also tested for nonlinearity using the generalized additive model with cubic splines for T and RH, which allowed for an estimation of flexible responses. The generalized additive model predicted that global partial and total effects did not improve over those of MLR (Supplementary Fig. 9).

Isolating CO_2 effect for ER. CLM5 simulates the enhancement effect of rising atmospheric CO_2 concentration on vegetation productivity through multiple CO_2-regulated processes in leaf photosynthesis for C_3 plants[55] and C_4 plants[56] and stomatal conductance[57]. To isolate and quantify the CO_2 fertilization effect for different crops in CLM5, an idealized scenario $RCP8.5_{(45CO2)}$ was designed that could represent a global warming scenario caused by greenhouse gases other than CO_2 that do not fertilize the vegetation growth (such as methane), while CO_2 emission was restrained or reduced. Through regression analysis based on $RCP8.5 - RCP8.5_{(45CO2)}$, the CO_2 fertilization effect was largely linear and exhibited a tendency towards acclimation when the CO_2 level was high (Extended Data Fig. 3). Thus, both linear and quadratic terms were used for CO_2 in the regression. The quadratic function estimated a hyperbolic response of crop yield to CO_2 enrichment, consistent with findings from FACE experiments[58]. The CO_2 regression coefficients for different crops were then compared with observations or other models (details in the main text).

The isolated climate-only effects (change in log yield based on $RCP4.5_{(SSP5LU)} - RCP8.5_{(45CO2)}$) and the effect of reduced CO_2 effect under ER (change in log yield based on $RCP8.5_{(45CO2)} - RCP8.5$) were then merged for each crop at each grid cell to estimate the total effect of ER (equivalent to $RCP4.5_{(SSP5LU)} - RCP8.5$ on a log scale). The partial and total effects of ER were then aggregated to regional or global average effects (and translated from a log scale to percentage effect) with the following procedure.

Resampling and aggregation. After decomposing the climate effects for SGs, and climate and CO_2 effects for ER per grid cell and finding the their global or regional means, we took a Monte Carlo or bootstrap approach (similar to Tai et al.[23]) to resampling the statistical predictions of partial and total effects at all participating grid cells for each crop 1,000 times to estimate their probability distribution for a region or the globe in each year under each scenario. At each time of resampling, a weighted-average method was applied to aggregate the grid-cell-level log effects (individual and compound effects of T, RD, RI, P and RH for SG or ER, and CO_2 for ER) per year to a region or the globe for each crop type using its crop area in each specific grid cell as the weight. The aggregated partial and total effects on a natural log scale were then translated to percentage effects per crop. The mean

and confidence interval of the individual effects of *T*, RD, RI, *P* and RH, their combinations (for example, RD + RI for radiation, *P* + RH for moisture) and the total effect on each crop were estimated from the resampling. Note that taking a different procedure, for example, translating from a log scale to per cent effect per grid cell before resampling and aggregation would bias the partial climate effects because $\exp\left(\sum\log\left(\frac{Y_i}{Y_c}\right)\right) \neq \sum\frac{Y_i}{Y_c}$.

To estimate global or regional average effects across all crop types, we weight-averaged the crop-specific percentage effects from the above steps using the product of the crop area and base yield of each crop as the weight, which takes into account the notable variations in base yield, as well as plot size across samples of different crop types (Supplementary Fig. 1). The total effect on the yields estimated from the above statistical prediction of the MLR, resampling and aggregation steps was also compared with the CLM modelled total effect (percentage change in global yield) under each SG (based on SAI/MSB/CCT – RCP8.5) or ER (RCP4.5$_{(SSP5LU)}$ – RCP8.5) to validate the statistical procedure. The difference between the MLR estimated total effect and CLM5 modelled total effect indicated the residual errors (Figs. 3 and 4). When the effect of LUC was considered in the alternative ER scenario, the climate-only effects from MLR, the CO_2 effect and the LUC effect were summed (on a log scale) at the grid-cell level followed by the same resampling and aggregation procedure to estimate the total effect for ER (Supplementary Sections 1 and 2 and Supplementary Fig. 3).

Small variations exist in the effective radiative forcing across the SG methods (Supplementary Table 1). After normalizing the effects of SGs using the scaling factors that match the mean and trend of the top-of-atmosphere radiative flux imbalance reduction by each SG to that of ER (Supplementary Figs. 10 and 11), the temperature and total effects of CCT become stronger than those of SAI, MSB and ER, but the overall advantage of SGs over ER and our main conclusions remain unchanged.

Reporting Summary. Further information on research design is available in the Nature Research Reporting Summary linked to this article.

Data availability

The intermediate data that support the findings of this study are available at https://doi.org/10.7910/DVN/Y1UHID. Source model data are available upon request from the corresponding author.

Code availability

Code for replicating the figures and analysis was written in R (version 3.6.2) or NCAR Command Language Version 6.5.0 and has been deposited in the Harvard Dataverse at https://doi.org/10.7910/DVN/Y1UHID. NorESM1-ME is available at https://github.com/NorESMhub/NorESM. CLM5 is available at https://github.com/ESCOMP/CTSM.

Received: 16 September 2020; Accepted: 16 April 2021;
Published online: 20 May 2021

References

1. Lawrence, M. G. et al. Evaluating climate geoengineering proposals in the context of the Paris Agreement temperature goals. *Nat. Commun.* **9**, 3734 (2018).
2. MacMartin, D. G., Ricke, K. L. & Keith, D. W. Solar geoengineering as part of an overall strategy for meeting the 1.5 °C Paris target. *Phil. Trans. R. Soc. A* **376**, 20160454 (2018).
3. Crutzen, P. J. Albedo enhancement by stratospheric sulfur injections: a contribution to resolve a policy dilemma? *Climatic Change* **77**, 211–220 (2006).
4. Ahlm, L. et al. Marine cloud brightening—as effective without clouds. *Atmos. Chem. Phys.* **17**, 13071–13087 (2017).
5. Muri, H. et al. Climate response to aerosol geoengineering: a multimethod comparison. *J. Clim.* **31**, 6319–6340 (2018).
6. Kravitz, B. et al. The Geoengineering Model Intercomparison Project (GeoMIP). *Atmos. Sci. Lett.* **12**, 162–167 (2011).
7. Robock, A., Oman, L. & Stenchikov, G. L. Regional climate responses to geoengineering with tropical and Arctic SO_2 injections. *J. Geophys. Res. Atmos.* **113**, D16101 (2008).
8. Tjiputra, J. F., Grini, A. & Lee, H. Impact of idealized future stratospheric aerosol injection on the large-scale ocean and land carbon cycles. *J. Geophys. Res. Biogeosci.* **121**, 2015JG003045 (2016).
9. Russell, L. M. et al. Ecosystem impacts of geoengineering: a review for developing a science plan. *Ambio* **41**, 350–369 (2012).
10. Xia, L. et al. Solar radiation management impacts on agriculture in China: a case study in the Geoengineering Model Intercomparison Project (GeoMIP). *J. Geophys. Res. Atmos.* **119**, 8695–8711 (2014).
11. Zhan, P., Zhu, W., Zhang, T., Cui, X. & Li, N. Impacts of sulfate geoengineering on rice yield in china: results from a multimodel ensemble. *Earth Future* **7**, 395–410 (2019).
12. Parkes, B., Challinor, A. & Nicklin, K. Crop failure rates in a geoengineered climate: impact of climate change and marine cloud brightening. *Environ. Res. Lett.* **10**, 084003 (2015).
13. Yang, H. et al. Potential negative consequences of geoengineering on crop production: a study of Indian groundnut. *Geophys. Res. Lett.* **43**, 11786–11795 (2016).
14. Pongratz, J., Lobell, D. B., Cao, L. & Caldeira, K. Crop yields in a geoengineered climate. *Nat. Clim. Change* **2**, 101–105 (2012).
15. Proctor, J., Hsiang, S., Burney, J., Burke, M. & Schlenker, W. Estimating global agricultural effects of geoengineering using volcanic eruptions. *Nature* **560**, 480–483 (2018).
16. Tjiputra, J. F. et al. Evaluation of the carbon cycle components in the Norwegian Earth System Model (NorESM). *Geosci. Model Dev.* **6**, 301–325 (2013).
17. MacMartin, D. G. & Kravitz, B. Mission-driven research for stratospheric aerosol geoengineering. *Proc. Natl Acad. Sci. USA* **116**, 1089–1094 (2019).
18. Lombardozzi, D. L. et al. Simulating agriculture in the community land model version 5. *J. Geophys. Res. Biogeosci.* **125**, e2019JG005529 (2020).
19. Popp, A. et al. Land-use futures in the shared socio-economic pathways. *Glob. Environ. Change* **42**, 331–345 (2017).
20. O'Neill, B. C. et al. The scenario model intercomparison project (ScenarioMIP) for CMIP6. *Geosci. Model Dev.* **9**, 3461–3482 (2016).
21. IPCC *Climate Change 2013: The Physical Science Basis* (eds Stocker, T. F. et al.) (Cambridge Univ. Press, 2013).
22. *FAOSTAT* (FAO, 2019); http://www.fao.org/faostat/en/?#data/QC
23. Tai, A. P. K., Martin, M. V. & Heald, C. L. Threat to future global food security from climate change and ozone air pollution. *Nat. Clim. Change* **4**, 817–821 (2014).
24. Hsiao, J., Swann, A. L. S. & Kim, S.-H. Maize yield under a changing climate: the hidden role of vapor pressure deficit. *Agric. For. Meteorol.* **279**, 107692 (2019).
25. Grossiord, C. et al. Plant responses to rising vapor pressure deficit. *New Phytol.* https://doi.org/10.1111/nph.16485 (2020).
26. Rigden, A. J., Mueller, N. D., Holbrook, N. M., Pillai, N. & Huybers, P. Combined influence of soil moisture and atmospheric evaporative demand is important for accurately predicting US maize yields. *Nat. Food* **1**, 127–133 (2020).
27. Konings, A. G., Williams, A. P. & Gentine, P. Sensitivity of grassland productivity to aridity controlled by stomatal and xylem regulation. *Nat. Geosci.* **10**, 284–288 (2017).
28. Novick, K. A. et al. The increasing importance of atmospheric demand for ecosystem water and carbon fluxes. *Nat. Clim. Change* **6**, 1023–1027 (2016).
29. Ainsworth, E. A. & Long, S. P. What have we learned from 15 years of free-air CO_2 enrichment (FACE)? A meta-analytic review of the responses of photosynthesis, canopy properties and plant production to rising CO_2: Tansley review. *New Phytol.* **165**, 351–372 (2004).
30. Bishop, K. A., Leakey, A. D. B. & Ainsworth, E. A. How seasonal temperature or water inputs affect the relative response of C_3 crops to elevated CO_2: a global analysis of open top chamber and free air CO_2 enrichment studies. *Food Energy Secur.* **3**, 33–45 (2014).
31. Ainsworth, E. A. et al. A meta-analysis of elevated CO_2 effects on soybean (*Glycine max*) physiology, growth and yield. *Glob. Change Biol.* **8**, 695–709 (2002).
32. Leakey, A. D. B. Rising atmospheric carbon dioxide concentration and the future of C_4 crops for food and fuel. *Proc. R. Soc. B* **276**, 2333–2343 (2009).
33. Ainsworth, E. A. & Rogers, A. The response of photosynthesis and stomatal conductance to rising CO_2: mechanisms and environmental interactions. *Plant Cell Environ.* **30**, 258–270 (2007).
34. National Research Council *Climate Intervention: Reflecting Sunlight to Cool Earth* (National Academies, 2015); https://doi.org/10.17226/18988
35. Lutsko, N. J., Seeley, J. T. & Keith, D. W. Estimating impacts and trade-offs in solar geoengineering scenarios with a moist energy balance model. *Geophys. Res. Lett.* **47**, e2020GL087290 (2020).
36. Friedlingstein, P. et al. Uncertainties in CMIP5 climate projections due to carbon cycle feedbacks. *J. Clim.* **27**, 511–526 (2014).
37. Tilmes, S. et al. The hydrological impact of geoengineering in the geoengineering model intercomparison project (GeoMIP). *J. Geophys. Res. Atmos.* **118**, 11,036–11,058 (2013).
38. Lawrence, D. M. et al. The community land model version 5: description of new features, benchmarking, and impact of forcing uncertainty. *J. Adv. Model. Earth Syst.* **11**, 4245–4287 (2019).
39. Fisher, R. A. et al. Parametric controls on vegetation responses to biogeochemical forcing in the CLM5. *J. Adv. Model. Earth Syst.* **11**, 2879–2895 (2019).
40. Bonan, G. B. et al. Model structure and climate data uncertainty in historical simulations of the terrestrial carbon cycle (1850–2014). *Glob. Biogeochem. Cycles* **33**, 1310–1326 (2019).
41. Osborne, T., Rose, G. & Wheeler, T. Variation in the global-scale impacts of climate change on crop productivity due to climate model uncertainty and adaptation. *Agric. For. Meteorol.* **170**, 183–194 (2013).

42. Peng, B. et al. Improving maize growth processes in the community land model: implementation and evaluation. *Agric. For. Meteorol.* **250–251**, 64–89 (2018).
43. Buzan, J. R. & Huber, M. Moist heat stress on a hotter earth. *Annu. Rev. Earth Planet. Sci.* **48**, 623–655 (2020).
44. Wieder, W. R. et al. Beyond static benchmarking: using experimental manipulations to evaluate land model assumptions. *Glob. Biogeochem. Cycles* **33**, 1289–1309 (2019).
45. Mercado, L. M. et al. Impact of changes in diffuse radiation on the global land carbon sink. *Nature* **458**, 1014–1017 (2009).
46. Cheng, S. J. et al. Variations in the influence of diffuse light on gross primary productivity in temperate ecosystems. *Agric. For. Meteorol.* **201**, 98–110 (2015).
47. Shao, L. et al. The fertilization effect of global dimming on crop yields is not attributed to an improved light interception. *Glob. Change Biol.* **26**, 1697–1713 (2020).
48. Vattioni, S. et al. Exploring accumulation-mode H_2SO_4 versus SO_2 stratospheric sulfate geoengineering in a sectional aerosol–chemistry–climate model. *Atmos. Chem. Phys.* **19**, 4877–4897 (2019).
49. Levis, S., Badger, A., Drewniak, B., Nevison, C. & Ren, X. CLMcrop yields and water requirements: avoided impacts by choosing RCP 4.5 over 8.5. *Climatic Change* **146**, 501–515 (2018).
50. Fricko, O. et al. The marker quantification of the Shared Socioeconomic Pathway 2: a middle-of-the-road scenario for the 21st century. *Glob. Environ. Change* **42**, 251–267 (2017).
51. Lauvset, S. K., Tjiputra, J. & Muri, H. Climate engineering and the ocean: effects on biogeochemistry and primary production. *Biogeosciences* **14**, 5675–5691 (2017).
52. Hurtt, G. C. et al. Harmonization of land-use scenarios for the period 1500–2100: 600 years of global gridded annual land-use transitions, wood harvest, and resulting secondary lands. *Climatic Change* **109**, 117–161 (2011).
53. West, T. O. et al. Cropland carbon fluxes in the United States: increasing geospatial resolution of inventory-based carbon accounting. *Ecol. Appl.* **20**, 1074–1086 (2010).
54. Lobell, D. B., Schlenker, W. & Costa-Roberts, J. Climate trends and global crop production since 1980. *Science* **333**, 616–620 (2011).
55. Farquhar, G., von Caemmerer, Svon & Berry, J. A biochemical model of photosynthetic CO_2 assimilation in leaves of C_3 species. *Planta* **149**, 78–90 (1980).
56. Collatz, G. J., Ribas-Carbo, M. & Berry, J. A. Coupled photosynthesis-stomatal conductance model for leaves of C_4 plants. *Funct. Plant Biol.* **19**, 519–538 (1992).
57. Medlyn, B. E. et al. Reconciling the optimal and empirical approaches to modelling stomatal conductance. *Glob. Change Biol.* **17**, 2134–2144 (2011).
58. Long, S. P., Ainsworth, E. A., Leakey, A. D. B., Nösberger, J. & Ort, D. R. Food for thought: lower-than-expected crop yield stimulation with rising CO_2 concentrations. *Science* **312**, 1918–1921 (2006).
59. *The NCAR Command Language (NCL, Version 6.5.0)* (UCAR, NCAR, CISL, TDD, 2018); https://doi.org/10.5065/D6WD3XH5

Acknowledgements

This study was supported by the Bjerknes Centre for Climate Research SKD-Fast Track Initiatives project (grant number 808011) and by Harvard University's Solar Geoengineering Research Program fellowship. J.T. was supported by the Research Council of Norway funded projects INES (grant number 270061) and COLUMBIA (grant number 275268). Y.F. and J.T. acknowledge funding from the European Commission, H2020 framework programme (CRESCENDO, grant number 641816). C.-E.P. was supported by Brain Pool Programs through the National Research Foundation of Korea (NRF) funded by the Ministry of Science and ICT (grant number 2019H1D3A1A01071022). The simulations were performed on resources provided by UNINETT Sigma2—the National Infrastructure for High Performance Computing and Data Storage in Norway, account numbers NS2345K and NS9033K. A. Grini provided original the SAI experimental settings in NorESM1-ME and P. Lawrence provided surface input data for CLM5. We also thank P. Irvine, J. Proctor, K. McColl and A. Berg for their helpful comments and communication on this work.

Author contributions

Y.F. and J.T. designed the study. Y.F. conducted the simulations and analysed the data with contributions from J.T., H.M. and D.L. H.M. provided the original MSB and CCT experimental settings. Y.F., J.T., H.M., D.L., C.-E.P., S.W. and D.K. interpreted the data and results. Y.F. wrote the first draft and all authors contributed to editing and revising the manuscript.

Competing interests

The authors declare no competing interests.

Additional information

Extended data is available for this paper at https://doi.org/10.1038/s43016-021-00278-w.

Supplementary information The online version contains supplementary material available at https://doi.org/10.1038/s43016-021-00278-w.

Correspondence and requests for materials should be addressed to Y.F.

Peer review information *Nature Food* thanks Thomas Leirvik, Peter Irvine and the other, anonymous, reviewer(s) for their contribution to the peer review of this work.

Reprints and permissions information is available at www.nature.com/reprints.

Publisher's note Springer Nature remains neutral with regard to jurisdictional claims in published maps and institutional affiliations.

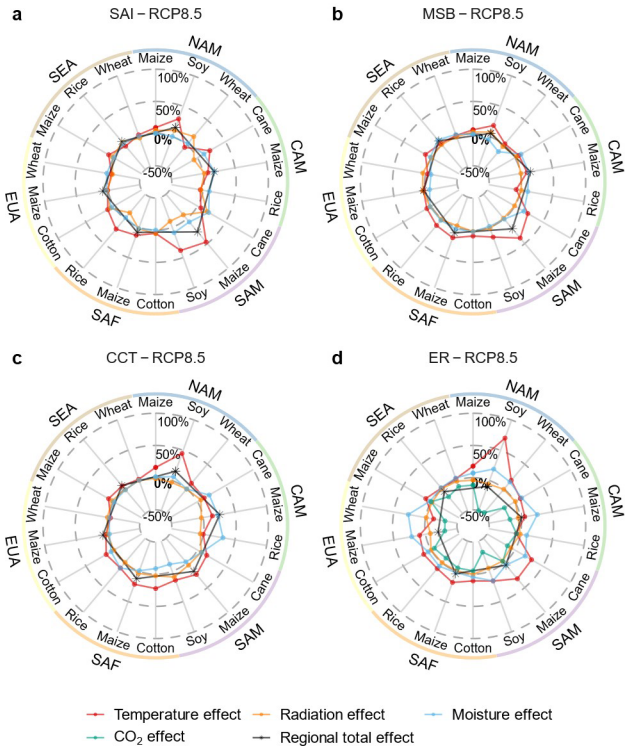

Extended Data Fig. 1 | Regional effects of SG or ER on selected main crops per region. a-d, Effects of temperature, radiation (direct and diffuse effects combined) and moisture (precipitation and relative humidity effects combined) on regional crop yield (crop-area weighted average; rainfed and irrigated proportions merged per crop) under SAI (**a**), MSB (**b**), CCT (**c**) and ER (with extra effect of CO_2; **d**) relative to RCP8.5. The black line depicts regional total effect on all six crops in each region, with the asterisks each representing one of the six regions defined in Fig.5. The colour lines represent the partial climate and CO_2 effects, with each point indicating one of three representative crops with largest cultivation areas in each region. Other minor crops for each region are shown in Extended Data Fig. 2. All values are averaged over the period of 2075–2099.

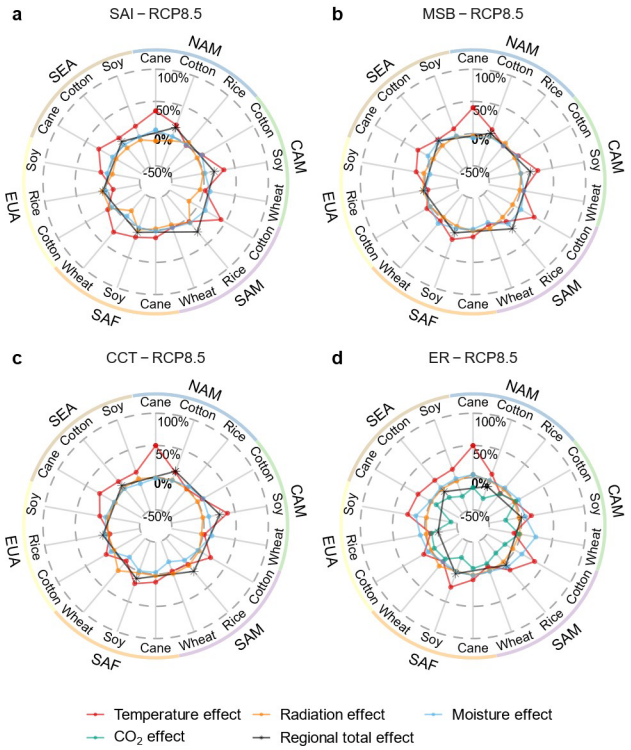

Extended Data Fig. 2 | Regional effects of SG or ER on other minor crops. a-d, Partial and total effects under SAI (**a**), MSB (**b**), CCT (**c**) and ER (**d**) as in Extended Data Fig. 1 but showing other minor crops existing in each of the six regions. Regional total effects of all six crops (black lines and asterisks) are identical to Extended Data Fig. 1.

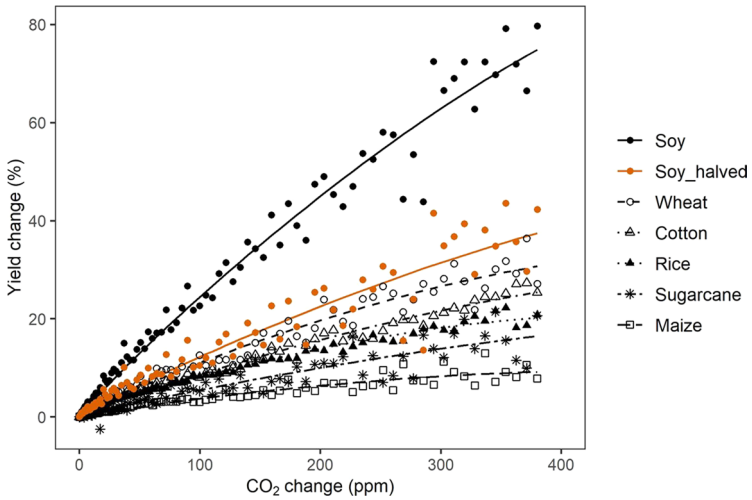

Extended Data Fig. 3 | Response of yield to changes in CO_2 concentration for each crop type. Points are prognostic yield difference against CO_2 difference between the experiments RCP8.5 and RCP8.5$_{(45CO2)}$ during 2006–2099. Lines are the predicted CO_2 effect using linear and quadratic coefficients from regression (see Methods). Red points and line indicate the modified yield change for soy when its CO_2 coefficients from regression are reduced by a factor of 2.

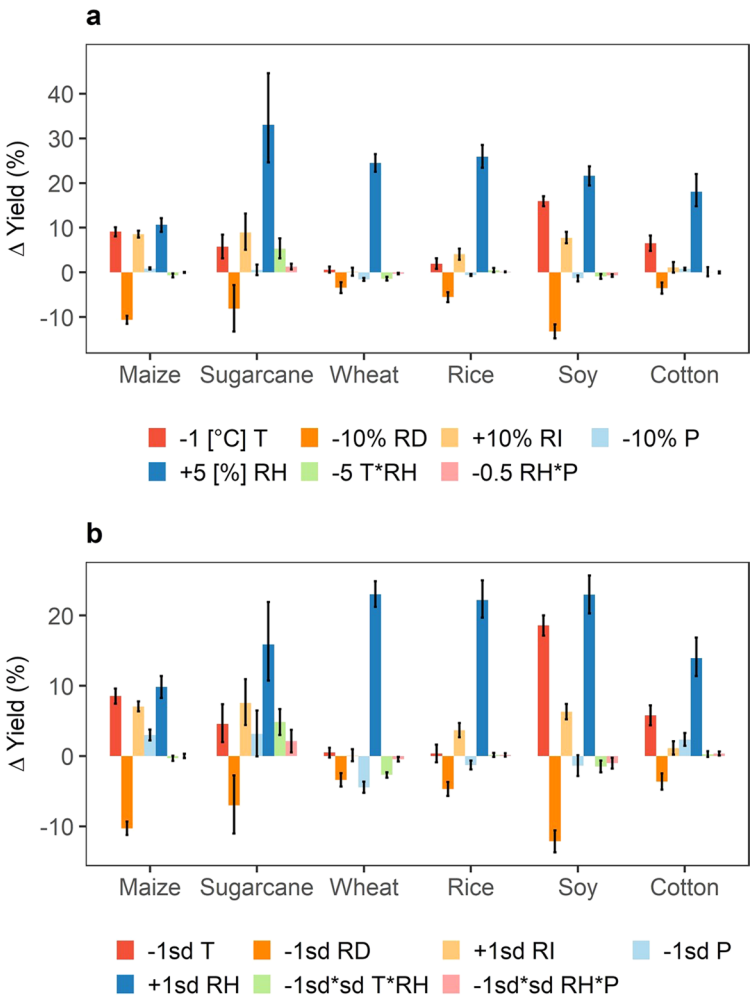

Extended Data Fig. 4 | Sensitivity of crop yields to unit changes in different climate variables under SAI estimated using the per-grid-cell MLR method. T, RD, RI, P and RH stand for temperature, direct radiation, diffuse radiation, precipitation and relative humidity, respectively. T*RH and RH*P indicate the interactions between T and RH and between RH and P, respectively. The regressions are refitted with log change in RD, RI and P so that their coefficients can be easily converted and applied to percentage changes in these variables and because these variables show log linear relationship with yield. **a**, Global average responses to unit changes applied uniformly to all grid cells (% indicates the native unit (percent) for relative humidity, but relative changes in the radiation terms). **b**, Global average response to a standard deviation (sd) of a variable for each crop grid cell under the scenario SAI – RCP8.5 during 2020–2099 (that is, sd is the local variability of climate change induced by SAI). Error bars indicate the 2.5th to 97.5th percentile confidence interval of the global average response from Bootstrap resampling and spatial aggregation.

nature research

Corresponding author(s): DBPR NATFOOD-20091526

Last updated by author(s): Sep 28, 2020

Reporting Summary

Nature Research wishes to improve the reproducibility of the work that we publish. This form provides structure for consistency and transparency in reporting. For further information on Nature Research policies, see our Editorial Policies and the Editorial Policy Checklist.

Statistics

For all statistical analyses, confirm that the following items are present in the figure legend, table legend, main text, or Methods section.

n/a	Confirmed	
☐	☒	The exact sample size (*n*) for each experimental group/condition, given as a discrete number and unit of measurement
☒	☐	A statement on whether measurements were taken from distinct samples or whether the same sample was measured repeatedly
☒	☐	The statistical test(s) used AND whether they are one- or two-sided *Only common tests should be described solely by name; describe more complex techniques in the Methods section.*
☐	☒	A description of all covariates tested
☐	☒	A description of any assumptions or corrections, such as tests of normality and adjustment for multiple comparisons
☐	☒	A full description of the statistical parameters including central tendency (e.g. means) or other basic estimates (e.g. regression coefficient) AND variation (e.g. standard deviation) or associated estimates of uncertainty (e.g. confidence intervals)
☒	☐	For null hypothesis testing, the test statistic (e.g. *F*, *t*, *r*) with confidence intervals, effect sizes, degrees of freedom and *P* value noted *Give P values as exact values whenever suitable.*
☒	☐	For Bayesian analysis, information on the choice of priors and Markov chain Monte Carlo settings
☒	☐	For hierarchical and complex designs, identification of the appropriate level for tests and full reporting of outcomes
☒	☐	Estimates of effect sizes (e.g. Cohen's *d*, Pearson's *r*), indicating how they were calculated

Our web collection on statistics for biologists contains articles on many of the points above.

Software and code

Policy information about availability of computer code

Data collection	NorESM1-ME, CLM5.0 (release-clm5.0.14)
Data analysis	NCAR Command Language (NCL) Version 6.5.0, R version 3.6.2

For manuscripts utilizing custom algorithms or software that are central to the research but not yet described in published literature, software must be made available to editors and reviewers. We strongly encourage code deposition in a community repository (e.g. GitHub). See the Nature Research guidelines for submitting code & software for further information.

Data

Policy information about availability of data

All manuscripts must include a data availability statement. This statement should provide the following information, where applicable:

- Accession codes, unique identifiers, or web links for publicly available datasets
- A list of figures that have associated raw data
- A description of any restrictions on data availability

The data that support the findings of this study are available from the corresponding author upon reasonable request. Source data for all figures will be made available in the public repository together with code.

Field-specific reporting

Please select the one below that is the best fit for your research. If you are not sure, read the appropriate sections before making your selection.

☐ Life sciences ☐ Behavioural & social sciences ☒ Ecological, evolutionary & environmental sciences

For a reference copy of the document with all sections, see nature.com/documents/nr-reporting-summary-flat.pdf

Ecological, evolutionary & environmental sciences study design

All studies must disclose on these points even when the disclosure is negative.

Study description	In this study we conducted climate simulations for three solar geoengineering scenarios (SAI, MSB, CCT) and two emissions scenarios (RCP4.5, RCP8.5) and crop simulations of six major crop types globally under each of the scenario. We then conducted spatial-temporal statistical analysis to isolate the effects of individual climate variables, CO2 and other factors on crop yield. A schematic figure (Fig. 1) and Table 1 in the main text and the Methods section provide details on the study design.
Research sample	Our research sample are model simulated global gridded annual crop yields for each of six crops maize, sugarcane, soy, rice, wheat and cotton (rainfed and irrigated separately, altogether 12 types) under each of five climate scenarios from 2020 to 2099 at 6641 unique crop-occupied grid cells, which together contribute to 23928 crop-grid specific regressions; each regression is based on a one-dimensional time series with sample size between 60 and 80.
Sampling strategy	We included the grid samples for each crop type if it occupies more than 1000 ha in each grid cell (a commonly used filter in references cited) for more than 60 years (to allow sufficient sample size) and have positive yields (to ensure valid values of log(yield)) in the multiple linear regression (MLR) analysis.
Data collection	Climate data were simulated by NorESM1-ME, which were used to drive crop yield simulations by CLM5.0. Global yield observations from 2006-2018 were obtained from the Food and Agricultural Organization of the United Nations corporate Statistical Database for model validation.
Timing and spatial scale	Our modeled yield data were produced at a spatial resolution of 1° (i.e., 192x288 grid cells globally) from the year 2006 to 2099 for RCP45 and RCP85 scenarios and 2020-2099 for the three solar geoengineering scenarios. The temporal resolution of model runs was 30-minute. Yield data were accumulated at annual time step.
Data exclusions	We only excluded grid cell samples for a specific crop if it occupies less than 1000 ha in each grid cell in a specific year (see Sampling strategy and more details in Methods).
Reproducibility	The model simulations could be largely reproduced following the same model settings using the same forcing data, but minor internal variability in the climate model could occur at each individual run. The NorESM1-ME model ensemble runs for each of the five climate scenarios considered in this study have been thoroughly analyzed in previous studies cited in this paper. The crop yield analysis and results can be reproduced using the code provided with this paper.
Randomization	Randomized allocation to control and treatment groups was not relevant in this modeling work as all grid samples were subject to multiple forcing variables simultaneously in the process-based global gridded crop model, but in the analysis grid samples for each crop type were compared with themselves over time (at least 60 years) with quasi-randomly assigned exposure to changing forcing conditions. Randomization is involved in our Monte Carlo/Bootstrap resampling (in Methods) to estimate the probability distribution of regression predicted partial and total climate effects.
Blinding	Blinding (and bias resulted from knowledge of group allocation) was not relevant in this study as crops and crop-occupied grid cells were the main subject and they were simulated simultaneously under the same process-based modeling framework and analysed equally in the same statistical procedure detailed above and in Methods.

Did the study involve field work? ☐ Yes ☒ No

Reporting for specific materials, systems and methods

We require information from authors about some types of materials, experimental systems and methods used in many studies. Here, indicate whether each material, system or method listed is relevant to your study. If you are not sure if a list item applies to your research, read the appropriate section before selecting a response.

Materials & experimental systems

n/a	Involved in the study
☒	☐ Antibodies
☒	☐ Eukaryotic cell lines
☒	☐ Palaeontology and archaeology
☒	☐ Animals and other organisms
☒	☐ Human research participants
☒	☐ Clinical data
☒	☐ Dual use research of concern

Methods

n/a	Involved in the study
☒	☐ ChIP-seq
☒	☐ Flow cytometry
☒	☐ MRI-based neuroimaging